1-1-2008

Double excitations and state-to-state transition dipoles in pi-pi* excited singlet states of linear polyenes: Time-dependent density-functional theory versus multiconfigurational methods

Ivan A. Mikhailov
University of Central Florida

Sergio Tafur
University of Central Florida

Artëm E. Masunov
University of Central Florida

Double excitations and state-to-state transition dipoles in π-π^* excited singlet states of linear polyenes: Time-dependent density-functional theory versus multiconfigurational methods

Ivan A. Mikhailov*
Nanoscience Technology Center, University of Central Florida, Orlando, Florida 32826, USA

Sergio Tafur
Nanoscience Technology Center and Department of Physics, University of Central Florida, Orlando, Florida 32826, USA

Artëm E. Masunov†
Nanoscience Technology Center, Department of Chemistry, and Department of Physics, University of Central Florida, Orlando, Florida 32826, USA

(Received 9 August 2007; published 24 January 2008)

The effect of static and dynamic electron correlation on the nature of excited states and state-to-state transition dipole moments is studied with a multideterminant wave function approach on the example of all-*trans* linear polyenes (C_4H_6, C_6H_8, and C_8H_{10}). Symmetry-forbidden singlet nA_g states were found to separate into three groups: purely single, mostly single, and mostly double excitations. The excited-state absorption spectrum is dominated by two bright transitions: $1B_u$-$2A_g$ and $1B_u$-mA_g, where mA_g is the state, corresponding to two-electron excitation from the highest occupied to lowest unoccupied molecular orbital. The richness of the excited-state absorption spectra and strong mixing of the doubly excited determinants into lower-nA_g states, reported previously at the complete active space self-consistent field level of theory, were found to be an artifact of the smaller active space, limited to π orbitals. When dynamic σ-π correlation is taken into account, single- and double-excited states become relatively well separated at least at the equilibrium geometry of the ground state. This electronic structure is closely reproduced within time-dependent density-functional theory (TD DFT), where double excitations appear in a second-order coupled electronic oscillator formalism and do not mix with the single excitations obtained within the linear response. An extension of TD DFT is proposed, where the Tamm-Dancoff approximation (TDA) is invoked after the linear response equations are solved (*a posteriori* TDA). The numerical performance of this extension is validated against multideterminant-wave-function and quadratic-response TD DFT results. It is recommended for use with a sum-over-states approach to predict the nonlinear optical properties of conjugated molecules.

DOI: 10.1103/PhysRevA.77.012510 PACS number(s): 31.10.+z, 32.70.Cs, 34.50.Gb, 31.15.E−

I. INTRODUCTION

Conjugated hydrocarbons (also known as polyenes) and their derivatives present an important class of compounds with rich photophysical and photochemical properties. These properties originate in highly polarizable π-electron systems and find wide use in organic electronics [1] and photonics [2] applications. Another reason for the interest in electronically excited states of polyenes is their role in biological processes of vision and photosynthesis. The theoretical description of electronic structure and electronic excited states in conjugated molecules plays a critical role in understanding natural and engineered processes, and may assist in the rational design of new materials with improved properties.

Polyenes often served as a testing ground for theoretical methods, and a comprehensive review of the published results seems to be an impossible venture. Presently, a consensus has been reached about the ordering of the lowest excited states, with the $2A_g$ state being above $1B_u$ (but close in energy) for all-*trans* butadiene and hexatriene and below the $1B_u$ state for the higher hydrocarbons. The transition dipole moments between excited states of polyenes have been much less studied, and the double-excited nature of $2A_g$ states is still a matter of discussion [3]. At the same time, the double-excited nature of selected excited states remains an important challenge of time-dependent density-functional theory (TD DFT) [4]. These aspects of electronic structure, as well as the ability of TD DFT methods to describe them, are the focus of this contribution.

Accurate numerical values of transition dipoles between excited states of molecules are important for predictions of nonlinear photonic processes [5,6], such as excited-state absorption and two-photon absorption. States involved in these processes are often not observable in linear absorption spectra and appear to possess a strong double-excited character [7–9]. The relation between two-photon absorption and other nonlinear optical (NLO) properties of ground sates is provided by the sum-over-states (SOS) expression, derived within the perturbation theory approach [10]. Several authors [11–13] noticed that the first and second hyperpolarizability values, obtained for the linear polyenes at semiempirical theory levels within the SOS approach, are dominated by contributions from a few, so-called "essential" states, so that all other states can be excluded from consideration. This approximation appeared attractive for structure-property relationship schemes [14,15], but later *ab initio* studies [16,17] reported it to be an oversimplification. In this contribution we reinvestigate the matter using a more advanced correla-

*On leave from Petersburg Nuclear Physics Institute, Gatchina, St. Petersburg 188300, Russia.
†Corresponding author. amasunov@mail.ucf.edu

tion treatment, analyze the structure of the higher excited states in details, and identify the approximations responsible for disagreements between different *ab initio* approaches.

II. THEORY

We aim to focus on the valence $\pi\pi^*$-excited states, which are primarily responsible for the second and higher polarizabilities of conjugated hydrocarbons. Linear all-*trans* polyenes are planar molecules of C_{2h} symmetry, their π orbitals belong to a_u and b_g irreducible representations. Configurations (Slater determinants) describing the electron transitions between the orbitals of the same symmetry contribute to A_g states, while transitions between the orbitals of different symmetry contribute to B_u states. Since the ground state is $1A_g$, one-photon transitions to B_u states are dipole allowed and to A_g states are dipole forbidden in the one-photon regime, while two-photon transitions are forbidden to B_u states and allowed to A_g states. Besides spatial symmetry, π states can be classified according to so-called alternacy, or particle-hole, symmetry [18]. It is exact only with some model Hamiltonians (Huckel or Parriser-Parr-Pople) and becomes approximate after σ-π and second-neighbor interactions are included. However, it is useful for an interpretation of transition dipoles from *ab initio* calculations.

Let us first introduce the shorthand notation $1,2,\ldots,m$ for the occupied and $1',2',\ldots,m'$ for the vacant π orbitals, with the highest occupied molecular orbital (HOMO) being 1 and the lowest unoccupied orbital (LUMO) being $1'$. When model Hamiltonians are used, the configurations $m\rightarrow n'$ and $n\rightarrow m'$ are degenerate and therefore contribute equally to the state wave function. Their in-phase and antiphase linear combinations give rise to *plus* and *minus* states [19]. The valence bond theory description of in-phase states [20] includes a substantial contribution from ionic resonance structures, while for the antiphase states it does not. For this reason *plus* and *minus* states are often called *ionic* and *covalent*, respectively [21]. The actual sign of the amplitude for every given configuration depends on the signs of singly occupied orbitals included in this configuration and is assigned arbitrarily in most software packages. Hence, we will use *ionic* and *covalent* notation, as *plus* and *minus* notation tends to be misleading. Similar to spatial symmetry, alternacy symmetry results in selection rules for one-photon transitions, as the dipole transition moment between any two *ionic* states or between any two *covalent* states is zero. The ground state $1A_g$ behaves like a *covalent* state. The excited configurations of the type $m\rightarrow m'$ behave like *ionic* states for singlet-spin states and *covalent* states for triplet-spin states. The doubly excited configurations of $mm\rightarrow n'n'$ type behave like *covalent* states and mix with the singly excited *covalent* configurations. This results in a multiconfigurational character of the *covalent* $2A_g$ state and explains why this state is strongly stabilized, sometimes below the *ionic* $1B_u$ state, of predominantly $1\rightarrow 1'$ nature.

An *ab initio* description of molecular excited states typically starts with molecular orbitals, optimized in a self-consistent field (SCF) procedure with a single Slater determinant wave function of the ground state, known as the restricted Hartree-Fock (HF) method. Excited states can in principle be described by single determinants (or two determinants, for open-shell singlets), which are constrained to be orthogonal to Slater determinants of the lower-lying states. While this approach works reasonably well at the DFT level [22,23], the HF description of excited states is generally inaccurate. Instead, configuration interaction (CI) methods are used, where one or more orbitals in the HF determinant are substituted with unoccupied orbitals to form excited configurations. The wave function of the system is expressed as a linear combination of these configurations, and electronic states are found by diagonalization of the Hamiltonian. All possible substitutions in the HF determinant (denoted excitation operators R in the following) yield the full configuration interaction [full CI (FCI)] method. It gives an exact solution to the Schrödinger equation for a given atomic basis [24]. The exponential growth of the computational effort with the size of the system makes FCI attainable only for very small molecular systems, and for practical reasons various truncation schemes are introduced. The simplest scheme restricts the expansion of the wave function to single substitutions [CI singles (CIS)]; another one limits the substitutions to singles and doubles (CISD). To reduce the computational effort, the amplitudes for double substitutions can be evaluated perturbatively (instead of the variational approach), resulting in the CIS(D) method [25]. When applied to the ground state, the method is known as MP2 (Møller-Plesset second-order perturbation) theory. Second-order algebraic diagrammatic construction [ADC(2)] presents yet another perturbation correction method, where the correction is applied to the matrix elements before solving CIS equations [26]. The variational CISD description for the ground state is known not to be size-consistent, which decreases its accuracy for dimers and larger molecules. In order to maintain size consistency, some of the higher excitations must be added to the wave function in the form of products of single and double-excited configurations. This approach results in coupled cluster expansions (CCSD, CC2, etc.) [27]. At the moment couple cluster methodology provides arguably the best accuracy/cost ratio among wave-function-based methods. CCSD expansion is applied to both ground and excited electronic states in symmetry-adapted cluster CI (SAC-CI) method [28,29]. The order of the general excitation operator R (defining a SAC-CI approximation level max R) can be limited to singles and doubles (max $R=2$, or SD-R) [30], or extended up to sixth-order (general-R) [29]. Both SD-R and general-R schemes were shown to yield similar results for the $2A_g$ state of *trans*-butadiene. This motivated us to adopt the SAC-CI (SD-R) method as a benchmark *ab initio* method in the present study.

Another truncation of the FCI wave function limits substitutions in the HF determinant to a small number of important orbitals, called the active space. When all substitutions within this active space are included in the wave function, the method is called the complete active space CI (CASCI) method. In addition, the SCF procedure can be used to optimize the orbitals for the state of interest, which constitutes the CASSCF method. In order to have a uniform description, the same set of orbitals is optimized sometimes for several states of interest [state-averaged (SA) CAS]. The limited active space describes the part of the electron correlation aris-

ing from the few nearly degenerate configurations (so-called *static electron correlation*). In order to account for *dynamic electron correlation*, originating from many higher-lying configurations, different extensions of the MP2 treatment to the CASSCF reference are introduced [complete active space second-order perturbation theory (CASPT2), multireference Møller-Plasset (MRMP), multireference quasidegenerate perturbation theory (MRQDPT), etc.]. As a more accurate and computationally demanding alternative, single and double excitations from the CAS reference can be included in the wave function variationally [multireference singles and doubles CI (MRD-CI)]. Size consistency is lost in MRD CI, but it can be approximately recovered *a posteriori* using Davidson's correction [31]. To reduce the computational demand, several elaborate techniques were introduced, including difference-dedicated CI (DDCI) [32] and the restricted-active-space method (RAS) [33]. Since the effect of electron correlation on ionic and covalent states is distinctly different, a balanced description of the valence excited states presents a challenge. As of 2004, only two state-of-the-art *ab initio* techniques (CASPT2 [34] and RASSCF [33]) were able to quantitatively reproduce the experimental [35] difference of −0.2 eV between vertical excitation energies to $1B_u$ and $2A_g$ states of hexatriene (Table S7 in Ref. [33]). Since CASPT2/ANO excitation energies are available for all the molecules considered in this contribution, they are used here for benchmarking purposes.

Unlike the electron correlation, the changes in the basis set seem to have a similar effect on *ionic* and *covalent* states. However, this effect is distinctly different from the effect on outervalent Rydberg states. Excited states of butadiene were studied with the CASPT2 and MRMP methods using both basis sets including [34] and excluding [36] diffuse and Rydberg functions. From a comparison of these studies [37], the energies of the valent $\pi\pi^*$ states are very similar and are not affected by the absence of diffuse and Rydberg functions. For this reason the basis sets DZp, TZ2p, and QZ3p, used by Nakayama *et al.* [36] (and obtained from correlation-consistent cc-pVXZ sets [38] by deleting the p functions on hydrogen and f,g functions on carbon atoms), were adopted in this study.

Detailed analysis of the wave function for higher polyenes (including hexatriene and octatetraene) was reported at the CASCI level [26] (while the corresponding excitation energies are reported at the CASCI MRMP level). According to this analysis, the ground $1A_g$ state has less than 15% and the lowest excited $2A_g$ state has close to 30% of double-excited character, regardless of the number of double bonds in the polyene. An even greater double-excited character (60%–80%) was obtained for a series of linear polyenes with the ADC(2) method [26]. At the same time the double-excited character of the ground $1A_g$ state obtained with the ADC(2) method increases linearly with the number of double bonds (10% for three bonds to 25% for seven bonds). From a comparison of CASCI-MRMP and CASPT2 studies one can notice that the choice of reference orbitals [restricted HF (RHF) or CASSCF] does not have a large effect on the state energies as long as dynamic correlation is taken into account. The double-excited character of the states is, however, strongly dependent on the method used. It is important to note that both the double-excited character and transition dipoles, reported in the works cited above, were evaluated with the CAS wave function (before dynamic correlation is taken into account). As will be discussed later, we found the effect of dynamic correlation to be critical.

Density functional theory in Kohn-Sham (KS) formalism [39] was the method of choice in solid-state theory for a long time. It received recognition as a reasonably accurate first-principles method for the ground states of large molecular systems after the generalized gradient approximation (GGA) was combined with a fraction of HF exchange (hybrid GGA) [40]. Instead of a multiconfigurational wave function, the KS DFT method accounts for electron correlation through the exchange-correlation potential. In particular, the contribution of double- and higher-excited configurations to the ground state is included in the single-Slater-determinant KS description implicitly. It was shown that the exact electron density obtained in multireference *ab initio* methods (such as full CI) can be mapped onto an effective single-particle KS description even for molecules far from equilibrium [41]. The ground-state wave function is simply not available in DFT for the analysis, and the single-determinant describes a hypothetical system of noninteracting electrons used in KS theory, rather than the molecular system of interest. Despite a single determinant appearance, DFT is not a single-reference method. This statement becomes apparent when Fermi broadening is applied to occupation numbers and these fractionally occupied KS orbitals are compared with natural orbitals, obtained in one of the wave-function-based methods [42]. From a practical standpoint, approximate hybrid exchange-correlation functionals (such as the Becke three-parameter Lee-Yang-Parr (B3LYP) hybrid functional [43]) produce energies close to coupled-cluster results in quality [40]. There are several extensions of DFT developed to describe the excited states. One approach is to use multireference strategies, described above [44–47]. More often, however, DFT is combined with a time-dependent perturbation theory approach, which we shall briefly describe next.

Instead of obtaining lowest-energy solutions to the Schrödinger equation based on the variational principle, the excited states can be described by a time-dependent perturbation theory treatment as the response of the molecular system to the external electric field [48]. Several formalisms have been developed to obtain excitation energies and transition dipoles directly [49], including equation-of-motion (EOM) and polarization propagator approaches. When the ground state is described with the HF method and terms higher than linear in external filed are neglected [linear response (LR)], the approach is called the time-dependent Hartree-Fock (TD HF) method, also known as the random phase approximation (RPA). When applied to the DFT ground state [50,51], the LR approximation is often called LR DFT, or TD DFT. The LR DFT method results in a non-Hermitian eigenvalue problem

$$\begin{pmatrix} A & B \\ -B & -A \end{pmatrix} \begin{bmatrix} X \\ Y \end{bmatrix} = \Omega \begin{bmatrix} X \\ Y \end{bmatrix}, \tag{1}$$

solution to which is the excitation energies Ω_α and transition density matrices ξ_α for the ground–to–excited-state transi-

tions. In the basis of occupied (i,j) and vacant (a,b) KS orbitals of σ,τ subsets $(\sigma,\tau=\alpha,\beta)$, the transition density is block diagonal with the occupied-vacant $X=(\xi)_{ia}$ and vacant-occupied $Y=(\xi)_{ai}$ blocks being nonzero. The matrices $\boldsymbol{A}$ and $\boldsymbol{B}$ are defined as

$$A_{ai\sigma,bj\tau}=\delta_{ab}\delta_{ij}\delta_{\sigma\tau}(\varepsilon_a-\varepsilon_i)+K_{ai\sigma,bj\tau},$$

$$B_{ai\sigma,bj\tau}=K_{ai\sigma,jb\tau}. \tag{2}$$

For the hybrid DFT with c_{HF} fraction of HF exchange, the coupling matrix $\boldsymbol{K}$ is expressed through the second derivatives of the exchange-correlation functional w and Coulomb and exchange integrals as

$$K_{ai\sigma,bj\tau}=(1-c_{\mathrm{HF}})(ia|w|jb)+(ia|jb)-c_{\mathrm{HF}}\delta_{\sigma\tau}(ab|ij). \tag{3}$$

The RPA or TD HF equation is then a limiting case with $c_{\mathrm{HF}}=1$, where the matrix $\boldsymbol{A}$ consists of interactions between two singly excited configurations $(a\leftarrow i|H|b\leftarrow j)$, also known as the CIS Hamiltonian. The matrix $\boldsymbol{B}$ includes, by virtue of swapping indices, the excitations from virtual to occupied molecular orbitals (MOs) (deexcitations) of the form $(a\leftarrow i|H|j\leftarrow b)$. Mathematically, they are equivalent to the matrix elements between the ground and doubly excited states [52]. Thus, LR DFT accounts for double excitations in two ways: implicitly, though the exchange-correlation functional, and explicitly, through the deexcitation matrix $\boldsymbol{B}$.

Sometimes an additional approximation is introduced in the LR formalism. It is called the Tamm-Dancoff approximation (TDA) [53,54] and consists in neglecting the deexcitation matrix $\boldsymbol{B}$ in Eq. (1). When applied to the HF ground state, it is equivalent to the configuration interaction method limited to singles (CIS). The double-excitation character is included in the TDA DFT formalism only implicitly through the approximate exchange-correlation (XC) potential. The TDA was found to be accurate when the exact XC potential was restored from the exact electron density in systems close to equilibrium [55] (but not when the covalent bond is stretched [4]). To a certain extent, the TDA may correct deficiencies in the approximate XC functionals [54].

In practice, an implicit account of double excitations was found to be more important than the role of the deexcitation matrix. For instance, a study of excited states in the radicals [56] demonstrated that TD DFT gives results comparable to the TD HF method for single-excited states and more accurate excitation energies for double-excited states. The results for linear polyenes were mixed. Several studies [3,37,57] reported correct state ordering only with pure XC functionals (and not with more accurate otherwise hybrid functionals), combined with the TDA and diffuse basis functions. Both successes and failures of LR DFT to describe potential energy surfaces of both single- and double-excited states, conical intersections between the states, and photochemical transformations have been reported [58–60].

Alternative approaches, taking one lowest double-excited state into account explicitly at the LR level, have been recently developed. Spin-flip DFT [61] and noncollinear XC with spin-flip excitations [62] methods use a $(\mathrm{HOMO})^1(\mathrm{LUMO})^1$ triplet as the reference state and obtain both ground and double-excited states as single excitations. Another approach, called dressed TD DFT [63], introduces frequency dependence into the exchange-correlation kernel (nonadiabatic approximation to TD DFT) by means of adding matrix elements involving double-excited $(\mathrm{HOMO})^2\rightarrow(\mathrm{LUMO})^2$ configurations into matrices $\boldsymbol{A}$ and $\boldsymbol{B}$ of Eq. (1). As a result, the $2A_g$ state acquires double-excited character and its energy is considerably lowered. Although double excitations could be included in extended or higher-order RPA formalisms [64], these methods have not received wide attention. Instead, the LR approximation has been applied to correlated ground states, including MCSCF [65], and CC [66–68].

We will next focus on transition dipole moments. In LR DFT they are readily obtained as a convolution of the dipole moment operator with the transition densities:

$$\mu_\alpha=\mathrm{Tr}(\mu\xi_\alpha). \tag{4}$$

State-to-state transition dipoles $\boldsymbol{\mu}_{\alpha,\beta}$ do not appear in the LR approximation, unless the excited state α is taken as the reference state. In order to obtain the expressions for $\boldsymbol{\mu}_{\alpha,\beta}$, one has to extend time-dependent perturbation theory to the quadratic response (QR). This extension was initially developed [69,70] for HF and MCSCF reference states using an explicit exponential unitary time-dependent transformation. The results of the perturbation treatment were expressed in terms of response functions (first-, second-, and third-order corrections to the expectation values of an arbitrary operator). Many molecular properties may be extracted form single and double residues of these response functions [71] at the resonant frequencies (poles of the response function). Specifically, the transition dipole between the excited states can be expressed through the ground-state dipole moment $\boldsymbol{\mu}_{o,o}$, ground–to–excited-state dipole moments $\boldsymbol{\mu}_\alpha$ and $\boldsymbol{\mu}_\beta$, and second residue of the dipole quadratic response function with two electric dipole perturbations $\boldsymbol{\mu}^b$ and $\boldsymbol{\mu}^c$ [70]:

$$\mu^a_{\alpha,\beta}=\mu^a_{0,0}\delta_{\alpha\beta}-(\mu^b_\alpha\mu^c_\beta)^{-1}\lim_{\omega_b\rightarrow-\omega_\alpha}\Big[\lim_{\omega_c\rightarrow\omega_\beta}(\omega_c-\omega_\beta)\times\langle\langle\mu^a;\mu^b,\mu^c\rangle\rangle\Big](\omega_b+\omega_\alpha). \tag{5}$$

Substitution of the LR values in place of dipoles evaluated with the exact states leads to summation over a large number of states. The explicit summation can be replaced by an iterative solution of the linear equations [70], which may be recast [72] in a form similar to Eq. (1). Luo *et al.* studied butadiene, hexatriene, and octatetraene at the QR HF level [16]. They found that the $1B_u$ state dominates the linear spectra, while three or four A_g states (depending on the basis set) that have large transition dipoles from the $1B_u$ state appear on two-photon absorption spectra with a maximum near 1.5–1.7 of the band gap (excitation energy of the $1B_u$ state). Quadratic response theory combined with DFT was also used for simulations of two-photon absorption spectra of other chromophores [73]. The quadratic response formalism, extended to CC [74] and DFT [75–77] reference states, is implemented using the DALTON suite of programs [78].

TABLE I. Excitation energies ΔE (eV) for the lowest π states of all-*trans* butadiene for the SAC-CI method (max$R$=4) with different basis sets in comparison with experiment and the best *ab initio* results [CAS PT2 with atomic natural orbitals (ANO) basis set].

	SAC-CI (max$R$=4)					CAS PT2	Experiment
Excited state	/DZp	/aug-DZp	/TZ2p	/aug-TZ2p	/QZ3p	/ANO	
$1B_u$	6.90	6.21	6.60	5.55	6.43	6.06,[a]6.23[b]	6.25,[c]5.92[d]
$2B_u$	11.77	10.20	11.17		10.90		
$2A_g$	7.46	6.90	7.28	6.34	7.19	6.27	
$3A_g$	9.40	8.00	8.88	7.41	8.63		
$4A_g$	12.54		12.47		12.19		

[a]Reference [84].
[b]Reference [34].
[c]Reference [85].
[d]Reference [86].

An alternative formulation of time-dependent perturbation theory for excited states is known as the coupled electronic oscillator (CEO) approach [79,80]. It uses a density matrix (Liouville space) representation and is based on the Heisenberg equation of motion for the ground-state density. It was recently extended from the HF to DFT reference state [81]. When only the terms of the first order in the external field are retained, Eq. (1), equivalent to the LR formalism, is obtained. In a second-order approximation, the solutions are sought in the basis of LR transition densities. As a result, linear excitations remain unchanged in the quadratic formalism and combined states $\boldsymbol{\xi}_\beta\boldsymbol{\xi}_\alpha$ of double-excited nature are added to the picture. The excitation energy for each of these new states is equal to the sum of single excitations:

$$\Omega_{\alpha\beta} = \Omega_\alpha + \Omega_\beta. \tag{6}$$

The second-order CEO gives the transition dipole between the ground and this double-excited state as

$$\mu_{0,\alpha\beta} = \sum_{\alpha\beta}^{perm} \mathrm{Tr}[\mu(I-2\rho)\xi_\alpha\xi_\beta] + \sum_{\gamma>0}\left(\frac{V_{\alpha\beta-\gamma}\mu_\gamma}{\Omega_\alpha+\Omega_\beta-\Omega_\gamma} - \frac{V_{\alpha\beta\gamma}\mu_{-\gamma}}{\Omega_\alpha+\Omega_\beta+\Omega_\gamma}\right). \tag{7}$$

Here the first summation runs over symmetrized permutations of the indices, the second summation runs over all excited states, $\mathbf{I}$ is the identity matrix, $\boldsymbol{\rho}$ is the ground-state density matrix, and $\mathbf{V}_{\alpha\beta-\gamma}$ is the exchange-correlation coupling term expressed via Kohn-Sham operators $V(\boldsymbol{\xi})$ on transition densities:

$$V_{\alpha\beta-\gamma} = \frac{1}{2}\sum_{\alpha\beta\gamma}^{perm} \mathrm{Tr}[(I-2\rho)\xi_\alpha\xi_\beta V(\xi_\gamma)]. \tag{8}$$

Further, the transition dipole between the double-excited state and any other excited state is zero unless the other state presents one of the components of this double-excited state:

$$\mu_{\alpha,\alpha\beta} = \mu_\beta, \quad \mu_{\alpha,\beta\gamma} = 0. \tag{9}$$

The transition dipole between two single-excited states is

$$\mu_{\alpha,\beta} = \sum_{-\alpha,\beta}^{perm} \mathrm{Tr}[\mu(I-2\rho)\xi_\alpha^*\xi_\beta] + \sum_{\gamma>0}\left(\frac{V_{-\alpha\beta-\gamma}\mu_\gamma}{-\Omega_\alpha+\Omega_\beta-\Omega_\gamma} + \frac{V_{\alpha-\beta-\gamma}\mu_{-\gamma}}{\Omega_\alpha-\Omega_\beta-\Omega_\gamma}\right). \tag{10}$$

Thus, in the second-order CEO the first double-excited state of $(\mathrm{HOMO})^2 \rightarrow (\mathrm{LUMO})^2$ type is always twice higher in energy than the HOMO→LUMO excited state and (unlike in wave-function-based methods), it never mixes with single excitations. The perturbative treatment can be further extended to correct the states, which leads to a mixing of single, double, and triple excitations within the TD DFT formalism [Eqs. (G5)–(G7) in Ref. [81]]:

$$\phi^{(0)} = |g\rangle_0 - \frac{1}{3!}\sum_{\alpha\beta\gamma>0}\frac{V_{-\alpha-\beta-\gamma}}{\Omega_\alpha+\Omega_\beta+\Omega_\gamma}a_\alpha^\dagger a_\beta^\dagger a_\gamma^\dagger|g\rangle_0, \tag{11}$$

$$\phi_\alpha^{(1)} = a_\alpha^\dagger|g\rangle_0 + \frac{1}{2!}\sum_{\beta\gamma>0}\frac{V_{\alpha-\beta-\gamma}}{\Omega_\alpha-\Omega_\beta-\Omega_\gamma}a_\beta^\dagger a_\gamma^\dagger|g\rangle_0, \tag{12}$$

$$\phi_{\beta\gamma}^{(2)} = a_\beta^\dagger a_\gamma^\dagger|g\rangle_0 + \frac{1}{2!}\sum_{\alpha>0}\frac{2V_{-\alpha\beta\gamma}}{-\Omega_\alpha+\Omega_\beta+\Omega_\gamma}a_\alpha^\dagger|g\rangle_0 + \frac{1}{2!}\sum_{\delta\zeta>0}\left(\frac{V_{\gamma-\delta-\zeta}}{\Omega_\gamma-\Omega_\delta-\Omega_\zeta}a_\beta^\dagger + \frac{V_{\beta-\delta-\zeta}}{\Omega_\beta-\Omega_\delta-\Omega_\zeta}a_\gamma^\dagger\right)a_\delta^\dagger a_\zeta^\dagger|g\rangle_0, \tag{13}$$

where $|g\rangle_0$, $a_\alpha^\dagger|g\rangle_0$, $a_\alpha^\dagger a_\beta^\dagger|g\rangle_0$, and $a_\alpha^\dagger a_\beta^\dagger a_\gamma^\dagger|g\rangle_0$ stand for the ground, single-, double-, and triple-excited states of the uncoupled system, respectively.

Double-excited states do not appear when the TDA is invoked, and exchange-correlation coupling terms $\mathbf{V}_{\alpha\beta-\gamma}$ vanish. As a result, state-to-state transition dipoles coincide with the ones obtained in the CIS method, defined by the first term of Eq. (10). One can also apply the TDA and annihilate the $\mathbf{Y}$ component of the transition density *a posteriori* after

the LR equation had been solved. Thus, excitation energies and ground–to–excited-state transition dipoles remain unaffected, while CIS formulas are applied to calculate state-to-state transition dipoles and differences between the unrelated and ground-state dipole moments:

$$\mu_{\alpha,\beta} = \mathrm{Tr}[\mu(I-2\rho)\xi^*_\alpha\xi_\beta],$$

$$\Delta\mu_\alpha = \mathrm{Tr}[\mu(I-2\rho)\xi^*_\alpha\xi_\alpha],$$

$$\xi = \begin{bmatrix} X \\ 0 \end{bmatrix}. \tag{14}$$

In addition, the double-excited states are introduced with the following excitation energies and transition dipoles:

$$\Omega_{\alpha\beta} = \Omega_\alpha + \Omega_\beta,$$

$$\mu_{0,\alpha\beta} = \mathrm{Tr}[\mu(I-2\rho)\xi_\alpha\xi_\beta],$$

$$\mu_{\alpha,\alpha\beta} = \mu_\beta, \quad \mu_{\alpha,\beta\gamma} = 0. \tag{15}$$

We will call this scheme the *a posteriori* Tamm-Dancoff (ATDA) approximation; it is intermediate between the TDA and full second-order TD DFT CEO. The ATDA allows one to calculate second-order properties without solving the equations of full QR DFT using a simple modification to existing LR codes. Unlike QR DFT, the ATDA inherits double-excited states from the second-order CEO formalism. In this contribution we examine the effect of the ATDA and TDA on transition dipoles between excited states and compare the numerical values with the ones obtained at higher theory levels.

III. COMPUTATIONAL DETAILS

For all SAC-CI and TD B3LYP calculations the GAUSSIAN 2003 suite of programs was used [82]. General-R, max$R$=2, and full-R generation options were used in the SAC-CI method to include double-excited states in the initial guess. SAC-CI excitation energies on CASSCF orbitals are obtained using a second job step with options SCF=MaxCycles=−1 Guess=read IOp(5/13=1, 8/42=10, 8/11=1, 8/46=1). State-to-state transition dipole moments at the ATDA B3LYP level were obtained with a locally modified version of the GAUSSIAN 2003 code. Properties of the double-excited states in the ATDA were coded according to formulas (14) and (15) and added to the list of LR states. Transition dipole moments at the QR-B3LYP level were calculated with DALTON 2.0 [78]. The basis sets DZp, TZ2p, and QZ3p, due to Nakayama *et al.* [36], were obtained by deleting the p,d functions on hydrogen and f,g functions on carbon from the correlation-consistent cc-pVXZ basis sets [38]. Diffused basis functions from aug-cc-pVXZ basis sets were used without alterations.

IV. RESULTS AND DISCUSSION

First, we verify the accuracy of the SAC-CI (SD-R) method to describe the valent excited states in butadiene. Several lowest excited $\pi\pi^*$ states are presented in Table I. Increasing the size of the basis set from DZp to TZ2p and QZ3p uniformly lowers the excitation energies by about 0.5 eV and essentially converges at QZ3p level, in agreement with MRMP results [36]. The remaining stabilization energy of the excited states (as compared to CASPT2/ANO [32]) is recovered when the basis set is augmented with diffused functions. However, diffused basis functions increase the computational costs for octatetraene beyond the present capabilities. Moreover, they complicate the wave function analysis and may result in appearance of intruder states [83]. For these reasons we limit the further discussion to the SAC-CI (SD-R)/DZp theory level, bearing in mind that it overestimates the excitation energies by about 1 eV for the lowest $\pi\pi^*$ states.

The results for the singlet $\pi\pi^*$ states of butadiene, hexatriene, and octatetraene are presented in Tables II–IV and Fig. 1. Comparison of the SAC-CI (max$R$=2) values for butadiene with the SAC-CI (max$R$=4) values from the first column in Table I shows that including the higher excited configurations (up to quadruple excitations) does not have any appreciable effect on the excitation energies in agreement with previously published SAC-CI results [28,29].

Close examination of the major configurations in the SAC-CI wave function reveals that alternacy symmetry classification into ionic and covalent states approximately holds. Out of two linear combinations of (i-j') and (j-i') determinants, the covalent combination is lower in energy and contains larger contribution from the double excitations. The actual signs of the amplitudes depend on the phase of the molecular orbitals and are therefore arbitrary. In Table III, for example, the ATDA B3LYP $2B_u$ and $3B_u$ states appear as minus and plus states, but are identified as covalent and ionic states, respectively based on excitation energies and transition dipole values. For covalent A_g states, one can observe the large transition dipole from the ionic $1B_u$ state. For covalent B_u states, transition dipoles from the covalent ground state are much lower than for ionic B_u states according to alternacy selection rules. As can be seen from the SAC-CI wave function analysis, this stabilization of the covalent versus ionic state corresponds to a 7%–14% contribution from the leading double-excited configuration, while this contribution is found to be insignificant in ionic states. The same stabilization is paralleled by both CIS(D) and TD DFT excitation energies. For instance, in hexatriene (Table III) the CIS covalent $2B_u$ state is 0.5 eV above the ionic $3B_u$ state and the CIS(D) covalent $2B_u$ state is 1.5 eV below the ionic $3B_u$ state. Similarly, the ATDA covalent $2B_u$ state is 1 eV lower than the ionic $3B_u$ state. While this stabilization is achieved through perturbative correction for double excitations in case of CIS(D), it is afforded by means of an exchange-correlation potential in the case of TD DFT. A comparison of SAC-CI with CIS results, where covalent states are systematically destabilized with respect to ionic states, is especially instructive.

Thus, analysis of the SAC-CI wave function, which includes both static and dynamic electron correlations, shows that the double-excited character of $2A_g$ and other lower-lying covalent states in the linear polyenes is relatively weak (less than 20%) and these states can be therefore classified

TABLE II. Excitation energies ΔE (eV), major contributing configurations, and % contributions of the leading double-excited configurations for the lowest π states of all-*trans* butadiene. Transition dipoles μ (a.u.) from the ground state to nB_u states and from $1B_u$ to nA_g states are also reported. All basis sets are DZp. The benchmark values of excitation energies obtained at CAS PT2/ANO are taken from Ref. [84].

	CIS		CIS(D)		SAC-CI (SD-*R*)			ATDA B3LYP			QR B3LYP	CAS PT2 /ANO
State	ΔE (eV)	Configurations	μ (a.u.)	ΔE (eV)	ΔE (eV)	Configurations	% *D*	μ (a.u.)	ΔE (eV)	Configurations	μ (a.u.)	μ (a.u.)	ΔE (eV)
$1B_u$	6.66	(1-1′)	2.661	6.77	6.86	(1-1′)	0	2.291	5.94	(1-1′)	2.131		6.06
$2B_u$	12.15	(2-2′)	0.784	11.33	11.72	(2-2′)+(11-1′2′)	2	0.874	10.33	(2-2′)	0.706		
$3B_u$			-	-	15.31	(11-1′2′)−(12-1′1′)	78	0.17	14.51	(1-1′)((1-2′)−(2-1′))			
$2A_g$	9.66	(1-2′)+(2-1′)	2.682	7.95	7.51	(2-1′)+(1-2′)+(11-1′1′)	13	1.695	7.11	(2-1′)+(1-2′)	1.485	1.293	6.27
$3A_g$	9.03	(1-2′)−(2-1′)	0.112	9.28	9.41	(1-2′)−(2-1′)	0	0.306	8.57	(1-2′)−(2-1′)	0.086	0.199	
$4A_g$			-	-	12.65	(2-1′)+(1-2′)−(11-1′1′)	53	2.698	11.89	(1-1′)(1-1′)	2.131		
$3A_g$			-	-	16.71	(12-1′2′)+(22-1′1′)+(11-2′2′)	83	0.557	16.28	(1-1′)(2-2′)	0.706		

TABLE III. Excitation energies ΔE (eV), major contributing configurations, and % contributions of the leading double-excited configurations for the lowest π states of all-*trans* hexatriene. Transition dipoles μ (a.u.) from the ground state to nB_u states and from $1B_u$ to nA_g states are also reported. All basis sets are DZp. The last column presents benchmark values of excitation energies at the CAS PT2/ANO theory level from Ref. [34]. Experimental values are given in parentheses.

	CIS		CIS(D)		SAC-CI (SD-*R*)			ATDA B3LYP			QR B3LYP	CAS PT2 /ANO
State	ΔE (eV)	Configurations	μ (a.u.)	ΔE (eV)	ΔE (eV)	Configurations	% *D*	μ (a.u.)	ΔE (eV)	Configurations	μ (a.u.)	μ (a.u.)	ΔE (eV)
$1B_u$	5.59	(1-1′)	2.353	5.62	5.58	(1-1′)	0	3.108	4.8	(1-1′)	2.986		5.01(4.95[a])
$2B_u$	9.57	(3-1′)+(1-3′)	0.130	7.76	7.28	(3-1′)+(1-3′)−(12-1′1′)+(11-1′2′)	12	0.075	7.04	(3-1′)−(1-3′)	0.032		
$3B_u$	9.05	(1-3′)−(3-1′)+(2-2′)	0.310	9.20	9.19	(3-1′)−(1-3′)	0	0.385	7.99	(1-3′)+(3-1′)	0.217		
$4B_u$	11.32	(2-2′)−(3-3′)	0.581	10.13	10.46	(2-2′)+(11-1′2′)−(13-1′2′)	5	0.946	8.86	(2-2′)	0.836		
$5B_u$	14.30	(2-2′)+(3-3′)	0.578	11.85	12.70	(3-3′)−(12-1′3′)+(13-1′2′)	5	0.868	11.06	(3-3′)	0.748		
$2A_g$	8.58	(1-2′)−(2-1′)	3.705	6.91	6.38	(2-1′)−(1-2′)+(11-1′1′)	12	2.758	5.81	(2-1′)+(1-2′)	2.172	1.767	5.19(5.21[b])
$3A_g$	7.99	(1-2′)+(2-1′)	0.779	7.90	8.08	(1-2′)+(2-1′)	0	0.415	7.18	(1-2′)−(2-1′)	0.262	0.244	
$4A_g$	13.89	(2-3′)+(3-2′)	0.387	10.84	10.45	(2-3′)+(3-2′)	8	0.478	9.47	(3-2′)+(2-3′)	0.194	2.890	
$5A_g$					11.12	(2-1′)−(1-2′)−(11-1′1′)	45	4.033	9.6	(1-1′)(1-1′)	3.108		
$6A_g$	11.67	(2-3′)−(3-2′)	0.105	10.73	11.16	(3-2′)−(2-3′)	1	0.144	9.9	(3-2′)−(2-3′)	0.031	0.290	

[a]Reference [87].
[b]Reference [88].

TABLE IV. Excitation energies ΔE (eV), major contributing configurations, and % contributions of the leading double-excited configurations for the lowest π states of all-*trans* octatetraene. Transition dipoles μ (a.u.) from the ground state to nB_u states and from $1B_u$ to nA_g states are also reported. The benchmark values of CAS PT2/ANO excitation energies in the last column are taken from Ref. [89].

CIS			CIS(D)	SAC-CI (SD-*R*)				ATDA-B3LYP			QR-B3LYP	CASPT2 /ANO
ΔE, eV	Configurations	μ (a.u.)	ΔE (eV)	ΔE (eV)	Configurations	% D	μ (a.u.)	ΔE (eV)	Configurations	μ (a.u.)	μ (a.u.)	ΔE (eV)
4.89	(1-1′)−(2-2′)	4.333	4.89	4.78	(1-1′)	0	3.108	4.09	(1-1′)	3.816		4.42
9.00	(1-3′)−(3-1′)	0.081	7.17	6.44	(3-1′)−(1-3′)−(12-1′1′)+(11-1′2′)	14	0.110	6.23	(3-1′)−(1-3′)	0.036		5.83
8.49	(1-3′)+(3-1′)+(2-2′)	0.780	8.40	8.37	(1-3′)+(3-1′)+(2-2′)	0	0.647	7.01	(2-2′)−(1-3′)	0.506		8.44
10.42	(2-2′)−(1-3′)	0.801	8.88	9.01	(2-2′)−(1-3′)+(11-1′2′)	2	0.901	7.70	(2-2′)+(1-3′)+(3-1′)	0.840		
11.38	(2-4′)−(4-2′)+(3-3′)	0.415	10.33	9.76	(2-4)+(4-2′)+(11-1′4′)+(14-1′1′)	11	0.013	8.95	(4-2′)+(2-4′)	0.016		
13.27	(2-4′)+(4-2′)	0.737	11.07	10.6	(4-2′)−(2-4′)+(14-1′1′)	1	0.435	9.43	(4-2′)−(2-4′)	0.206		
13.54	(4-2′)+(4-4′)	0.894	11.07	11.49	(3-1′)−(1-3′)+(12-1′1′)−(11-1′2′)	44	0.054	10.29	(1-1′)((2-1′)−(1-2′))			
7.71	(1-2′)+(2-1′)	4.505	6.03	5.22	(2-1′)+(1-2′)+(11-1′1′)	12	3.243	4.90	(2-1′)+(1-2′)	2.777	2.197	4.38
7.12	(1-2′)−(2-1′)	0.947	6.92	6.61	(2-1′)−(1-2′)	0	0.468	6.20	(1-2′)−(2-1′)	0.304	0.221	6.56
9.50	(4-1′)−(1-4′)	0.376	7.79	6.77	(1-4′)−(4-1′)−(13-1′1′)−(11-1′3′)	11	0.263	6.92	(1-4′)−(4-1′)	0.229	0.448	7.14
8.95	(1-4′)−(2-3′)	0.147	8.90	8.55	(1-4′)+(4-1′)−(24-1′1′)(13-1′1′)	2	0.243	7.72	(1-4′)+(4-1′)	0.024	0.232	
-		-	-	9.41	(1-2′)+(2-1′)−(11-1′1′)	41	5.340	8.17	(1-1′)(1-1′)	3.816		
11.23	(2-3′)−(3-2′)	0.038	9.99	9.93	(3-2′)−(2-3′)−(11-1′3′)	2	0.108	8.31	(2-3′)+(3-2′)	0.285	4.360	
15.91	(3-4′)−(4-3′)	0.078	12.56	11.34	(3-4′)+(22-1′3′)	5	0.436	10.43	(3-4′)	0.031	10.521	
13.83	(3-4′)+(4-3′)	0.019	11.61	11.75	(3-4′)−(4-3′)−(2-3′)+(13-1′1′)	7	0.496	10.77	(4-3′)	0.024	0.000	
12.67	(3-2′)+(2-3′)	0.490	12.67	11.91	(3-2′)+(2-3′)+(4-3′)+(13-1′1′)	6	0.556	8.97	(2-3′)−(3-2′)	0.035	9.535	
-		-	-	12.86	(4-1′)−(1-4′)+(12-1′2′)+(11-1′3′)+(13-1′1′)	61	0.694	11.10	(1-1′)((2-2′)−(1-3′)+(3-1′))	0.506		

as predominantly single excitations. This is in contrast with ionic states that have purely single-excited character. Some of the higher-lying states, however, have considerably higher contributions of the doubly excited configurations (40%–80%). Excitation energies of these states are close to the sum of the excitation energies of the respective predominantly single-excited states. Even though doubly excited configurations appear to contribute much less than 100% to the wave function, this contribution is more than twice greater than the one observed in predominantly single-excited states. Thus, these states can be interpreted as predominantly double excited. This interpretation is confirmed by the trends in excitation energy and transition dipoles, as described below. Thus, single and double excitations in linear polyenes at equilibrium geometry are separated by a gap in double-excited character (below 20% and above 40%). It is conceivable that far from equilibrium geometry this observation may no longer hold.

Let us consider the $4A_g$ state of butadiene as an example. According to the Table II, $4A_g$ has excitation energy of 12.6 eV, approximately twice the excitation energy for $2B_u$ state (6.8 eV). Meanwhile, its leading configuration (11-1′1′) corresponds to the double HOMO-LUMO excitation (1-1′), which is the leading configuration in the $2B_u$ state. Similarly, the $3B_u$ state of butadiene with leading configurations of (11-1′2′)−(12-1′1′) originates from the product of singly excited $1B_u$ (1-1′) and $3A_g$ (1-2′)−(2-1′) states. Its excitation energy of 15.3 eV is nearly equal to the sum of the respective excitation energies of 6.8 and 9.4 eV.

The relationships observed in SAC-CI results are closely resembled by the ATDA B3LYP level of theory. The $2A_g$ and other states, found to be predominantly single excitations with the SAC-CI method, were found to have excitation energies closer to benchmark values than uncorrected SAC-CI/DZp values. Unlike CIS(D) and SAC-CI results, covalent states are stabilized relative to the corresponding ionic states without explicitly including double-excited configurations in the description. This confirms that the same electron correlation effects, which are described by double-excited configurations in the wave function, are accounted for by the approximate exchange-correlation functional B3LYP. On the other hand, the states, interpreted as predominantly doubly excited, are well reproduced by the second-order CEO extension to TD DFT, after Eqs. (6)–(10) are simplified with an *a posteriori* Tamm-Dancoff approximation. These states are completely absent in the list of CIS and CIS(D) states. It is necessary to stress that double-excited states are not present in the output of standard computer codes implementing TD DFT in both linear or quadratic response.

Transition dipole moments calculated with ATDA DFT are in better agreement with SAC-CI values than CIS ones. They also compare favorably with QR DFT results. While ground to B_u transition dipole moments are the same in the ATDA and QR DFT methods (being LR values), $1B_u$ to nA_g transition dipoles are different. Ionic states are almost equally dark with the QR and ATDA. Covalent A_g states of mostly single-excited character are bright in the SAC-CI model, darker with the ATDA, and even darker with the QR. Covalent states of mostly double-excited character are com-

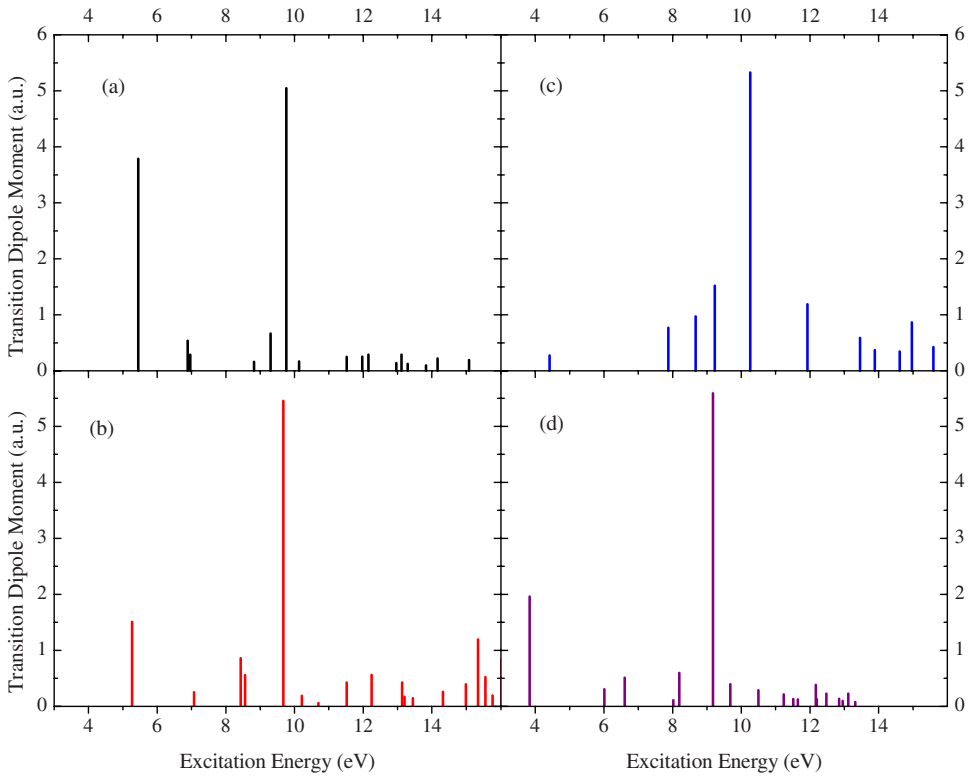

FIG. 1. (Color online) Transition dipole moments from the $1B_u$ state to the manifold of nA_g excited states of all-*trans* octatetraene with excitation energies below 16 eV calculated using different active orbital space: (a) SAC-CI method (max$R$=2) in full RHF orbital space (default option for SAC); (b) SAC-CI method (max$R$=2) in π-only active RHF orbital subspace; (c) SAC-CI method (max$R$=4) in π-only active SA CASSCF(8,8) subspace, averaged over $1A_g$, $1B_u$, and $2A_g$ states; and (d) SAC-CI method (max$R$=4) in full SA CASSCF(8,8) space.

pletely absent in the QR, but their transition dipoles are borrowed by other states close in energy. In octatetraene as many as four states borrow their intensity from this missing double excitation and need to be summed together for fair comparison with the SAC-CI values. Even with this in mind, ATDA values are still closer to SAC-CI ones. According to Eq. (9), the transition dipole moment between the single- and double-excited states (including this singly excited state as its component) is equal to the one from the ground to the second component of the double-excited state. SAC-CI transition dipole values between respective states are close to this CEO relationship, which confirms our classification of covalent states into predominantly single and predominantly double excitations.

The SAC-CI results on the double-excited character and transition dipoles are somewhat in disagreement with CASSCF and CASCI data, cited previously. In order to investigate the differences between SAC-CI and CASSCF wave functions and transition diploes, we plotted $1B_u$-nA_g transition dipoles for octatetraene, using the standard SAC-CI (max$R$=2) method [Fig. 1(a)] and SAC-CI (max$R$=2) methods with only four π and four lowest π^* orbitals in the correlated window [Fig. 1(b)]. While only two states ($2A_g$ and the first predominantly doubly excited $6A_g$) dominate the SAC-CI picture obtained in full orbital space, the $2A_g$ becomes less important and other states become more important. This trend is much more pronounced when RHF orbitals (used by default in the SAC-CI method), were replaced with the orbitals optimized by state-averaged CASSCF method [Fig. 1(c)], similar to the protocol used by Beljonne *et al.* [17] Along with the drastic reduction of the transition-state dipole moment, the double-excitation character of the $2A_g$ state increased to 24%. Both observations are in agreement with published CASSCF results. Finally, when all CASSCF orbitals are used in the SAC-CI (max$R$=4) treatment [Fig. 1(d)], the picture closely resembles the original one, with only two essential mA_g states remaining.

Thus, we established that restricting the active space to π orbitals only and optimizing them with state-average technique increases both the mixing of the double-excited configuration with single-excited ones and introduces drastic distortions into the transition dipole moment values. The richness of the excited-state absorption spectrum, reported previously, turns out to be an artifact of the neglected dynamic electron correlation by using a limited active orbital space. According to the full orbital-space SAC-CI method, the absorption spectrum of the $1B_u$ state in octatetraene is dominated by the $2A_g$ state and higher-mA_g state with twice as large transition dipole and energy nearly twice the band gap (i.e., energy of the $1B_u$ state). This is well reproduced by the second-order TD DFT CEO formalism, approximated by the ATDA method.

V. CONCLUSIONS

In this contribution singlet excited states in the short linear polyenes are studied with a wave-function-based

method SAC-CI, including a description of both static and dynamic electron correlation. A_g states are found to separate into three groups: purely single, mostly single, and mostly double excitations. The first excited-state absorption spectrum is dominated by two bright transitions $1B_u$-$2A_g$ and $1B_u$-mA_g, where mA_g is a $(\mathrm{HOMO})^2$-$(\mathrm{LUMO})^2$ transition. Multiple bright states reported previously for the excited state absorption spectra at the CASSCF level and used to invalidate the essential states models are now found to be an artifact of the limited active orbital space. A variation of the second-order TD DFT method, named the *a posteriori* Tamm-Dancoff approximation, was proposed. It consists of solving the full linear response equations [Eqs. (1)–(4)], evaluation of the difference permanent and state-to-state transition dipoles with Eq. (14), and calculation of excitation energies and transition dipoles for double-excited states as combinations of respective linear response values according to Eq. (15).

When our definition of predominantly double excitation is used (above 40% contribution of the double-excited configuration), excited states of linear polyenes at equilibrium geometry do not present a continuous mix of single and double excitations. This however may happen away from equilibrium, such as transition states to isomerization and conical intersections. One would expect that mixing of singly and doubly excited states according to Eqs. (11)–(13) may describe excited states better than the ATDA in those cases.

For the equilibrium geometries considered here, the ATDA DFT numerical results were found to be in better agreement with SAC-CI values than QR DFT ones. We recommend ATDA DFT for calculation of the nonlinear optical properties of conjugated chromophores. This work is presently underway.

ACKNOWLEDGMENTS

This work was supported in part by National Science Foundation Grant No. CCF 0740344. The authors are thankful to DOE NERSC and UCF I2Lab for the generous donation of computer time. S.T. gratefully acknowledges support by the UCF NSTC.

[1] H. E. Katz, Chem. Mater. **16**, 4748 (2004).
[2] L. R. Dalton, J. Phys.: Condens. Matter **15**, R897 (2003).
[3] J. H. Starcke, M. Wormit, J. Schirmer *et al.*, Chem. Phys. **329**, 39 (2006).
[4] J. Neugebauer, E. J. Baerends, and M. Nooijen, J. Chem. Phys. **121**, 6155 (2004).
[5] J. W. Perry, S. R. Marder, F. Meyers *et al.*, in *Polymers for Second-Order Nonlinear Optics*, edited by G. A. Sindsay and K. D. Singer (American Chemical Society, Washington, D.C., 1995), Vol. 601, p. 45.
[6] K. Y. Suponitsky, T. V. Timofeeva, and M. Y. Antipin, Usp. Khim. **75**, 515 (2006).
[7] K. Schulten and M. Karplus, Chem. Phys. Lett. **14**, 305 (1972).
[8] R. Olchawa, Physica B **291**, 29 (2000).
[9] W. Barford, R. J. Bursill, and M. Y. Lavrentiev, Phys. Rev. B **63**, 195108 (2001).
[10] B. J. Orr and J. F. Ward, Mol. Phys. **20**, 513 (1971).
[11] J. W. Wu *et al.*, J. Opt. Soc. Am. B **6**, 707 (1989).
[12] P. C. M. McWilliams, G. W. Hayden, and Z. G. Soos, Phys. Rev. B **43**, 9777 (1991).
[13] D. Guo, S. Mazumdar, S. N. Dixit, F. Kajzar, F. Jarka, Y. Kawabe, and N. Peyghambarian, Phys. Rev. B **48**, 1433 (1993).
[14] W. L. Fitch *et al.*, J. Chem. Inf. Comput. Sci. **42**, 830 (2002).
[15] M. Rumi *et al.*, J. Am. Chem. Soc. **122**, 9500 (2000).
[16] Y. Luo, H. Agren, and S. Stafstrom, J. Phys. Chem. **98**, 7782 (1994).
[17] D. Beljonne *et al.*, Chem. Phys. Lett. **279**, 1 (1997).
[18] T. Hashimoto, H. Nakano, and K. Hirao, J. Chem. Phys. **104**, 6244 (1996).
[19] R. Pariser, J. Chem. Phys. **24**, 250 (1956).
[20] K. Hirao *et al.*, J. Chem. Phys. **105**, 9227 (1996).
[21] J. P. Malrieu, I. Nebotgil, and J. Sanchezmarin, Pure Appl. Chem. **56**, 1241 (1984).
[22] V. N. Glushkov, Opt. Spectrosc. **99**, 684 (2005).
[23] S. R. Billeter and D. Egli, J. Chem. Phys. **125**, 224103 (2006).
[24] P.-O. Löwdin and H. Shull, Phys. Rev. **101**, 1730 (1956).
[25] M. Headgordon *et al.*, Chem. Phys. Lett. **219**, 21 (1994).
[26] Y. Kurashige *et al.*, Chem. Phys. Lett. **400**, 425 (2004).
[27] H. Sekino and R. J. Bartlett, in *Advances in Quantum Chemistry*, edited by P.-O. Lowden (Academic Press Inc., San Diego, 1999), Vol. 35, p. 149.
[28] H. Nakatsuji, Chem. Phys. Lett. **177**, 331 (1991).
[29] B. Saha, M. Ehara, and H. Nakatsuji, J. Chem. Phys. **125**, 014316 (2006).
[30] O. Kitao and H. Nakatsuji, Chem. Phys. Lett. **143**, 528 (1988).
[31] S. R. Langhoff and E. R. Davidson, Int. J. Quantum Chem. **8**, 61 (1974).
[32] J. Cabrero, R. Caballol, and J. P. Malrieu, Mol. Phys. **100**, 919 (2002).
[33] M. Boggio-Pasqua *et al.*, J. Chem. Phys. **120**, 7849 (2004).
[34] L. Serrano-Andres *et al.*, J. Chem. Phys. **98**, 3151 (1993).
[35] R. M. Gavin, S. Risember, and S. A. Rice, J. Chem. Phys. **58**, 3160 (1973).
[36] K. Nakayama, H. Nakano, and K. Hirao, Int. J. Quantum Chem. **66**, 157 (1998).
[37] C. P. Hsu, S. Hirata, and M. Head-Gordon, J. Phys. Chem. A **105**, 451 (2001).
[38] T. H. Dunning, J. Chem. Phys. **90**, 1007 (1989).
[39] W. Kohn and L. J. Sham, Phys. Rev. **140**, A1133 (1965).
[40] C. Adamo, A. di Matteo, and V. Barone, in *Advances in Quantum Chemistry*, editedP.-O. Lowden (Academic Press Inc., San Diego, 2000), Vol. 36, p. 45.
[41] O. V. Gritsenko and E. J. Baerends, Theor. Chem. Acc. **96**, 44 (1997).
[42] R. Takeda, S. Yamanaka, and K. Yamaguchi, Int. J. Quantum Chem. **101**, 658 (2005).

[43] A. D. Becke, J. Chem. Phys. **107**, 8554 (1997).
[44] S. Grimme and M. Waletzke, J. Chem. Phys. **111**, 5645 (1999).
[45] S. Grimme, J. Chem. Phys. **124**, 034108 (2006).
[46] S. Yamanaka *et al.*, Chem. Lett. **35**, 242 (2006).
[47] C. Gutle and A. Savin, Phys. Rev. A **75**, 032519 (2007).
[48] P. W. Langhoff, S. T. Epstein, and M. Karplus, Rev. Mod. Phys. **44**, 602 (1972).
[49] A. E. Hansen and T. D. Bouman, Mol. Phys. **37**, 1713 (1979).
[50] E. Runge and E. K. U. Gross, Phys. Rev. Lett. **52**, 997 (1984).
[51] M. E. Casida, in *Recent Advances in Density-Functional Methods*, edited by D. P. Chong (World Scientific, Singapore, 1995), Pt. 1, Vol. 3.
[52] R. E. Stratmann, G. E. Scuseria, and M. J. Frisch, J. Chem. Phys. **109**, 8218 (1998).
[53] T. H. Dunning and V. McKoy, J. Chem. Phys. **47**, 1735 (1967).
[54] S. Hirata and M. Head-Gordon, Chem. Phys. Lett. **314**, 291 (1999).
[55] A. Savin, C. J. Umrigar, and X. Gonze, Chem. Phys. Lett. **288**, 391 (1998).
[56] S. Hirata and M. Head-Gordon, Chem. Phys. Lett. **302**, 375 (1999).
[57] J. Catalan and J. L. G. de Paz, J. Chem. Phys. **120**, 1864 (2004).
[58] M. Wanko *et al.*, J. Chem. Phys. **120**, 1674 (2004).
[59] B. G. Levine *et al.*, Mol. Phys. **104**, 1039 (2006).
[60] S. Fantacci, A. Migani, and M. Olivucci, J. Phys. Chem. A **108**, 1208 (2004).
[61] Y. H. Shao, M. Head-Gordon, and A. I. Krylov, J. Chem. Phys. **118**, 4807 (2003).
[62] J. G. Guan *et al.*, J. Chem. Phys. **125**, 044314 (2006).
[63] N. T. Maitra *et al.*, J. Chem. Phys. **120**, 5932 (2004).
[64] T. Shibuya, J. Rose, and V. McKoy, J. Chem. Phys. **58**, 500 (1973).
[65] P. Jorgensen *et al.*, Int. J. Quantum Chem. **23**, 959 (1983).
[66] S. Hirata *et al.*, J. Chem. Phys. **114**, 3919 (2001).
[67] J. F. Stanton and R. J. Bartlett, J. Chem. Phys. **98**, 7029 (1993).
[68] J. E. DelBene, J. D. Watts, and R. J. Bartlett, J. Chem. Phys. **106**, 6051 (1997).
[69] E. Dalgaard, J. Chem. Phys. **72**, 816 (1980).
[70] J. Olsen and P. Jorgensen, J. Chem. Phys. **82**, 3235 (1985).
[71] O. Vahtras *et al.*, J. Chem. Phys. **97**, 9178 (1992).
[72] K. Sasagane, F. Aiga, and R. Itoh, J. Chem. Phys. **99**, 3738 (1993).
[73] P. Salek *et al.*, Chem. Phys. Lett. **374**, 446 (2003).
[74] E. Dalgaard and H. J. Monkhorst, Phys. Rev. A **28**, 1217 (1983).
[75] H. Larsen *et al.*, J. Chem. Phys. **113**, 8908 (2000).
[76] F. Furche, J. Chem. Phys. **114**, 5982 (2001).
[77] P. Salek *et al.*, J. Chem. Phys. **117**, 9630 (2002).
[78] P. Cronstrand, Y. Luo, and H. Agren, in *Advances in Quantum Chemistry*, editedJ. R. Sabin and E. Brändas (Elsevier Academic Press Inc., San Diego, 2005), Vol. 50, p. 1.
[79] J. Knoester and S. Mukamel, Phys. Rev. A **39**, 1899 (1989).
[80] S. Tretiak and S. Mukamel, Chem. Rev. **102**, 3171 (2002).
[81] S. Tretiak and V. Chernyak, J. Chem. Phys. **119**, 8809 (2003).
[82] GAUSSIAN 03, Revision D.01, M. J. Frisch, G. W. Trucks, H. B. Schlegel, G. E. Scuseria, M. A. Robb, J. R. Cheeseman, J. A. Montgomery, Jr., T. Vreven, K. N. Kudin, J. C. Burant, J. M. Millam, S. S. Iyengar, J. Tomasi, V. Barone, B. Mennucci, M. Cossi, G. Scalmani, N. Rega, G. A. Petersson, H. Nakatsuji, M. Hada, M. Ehara, K. Toyota, R. Fukuda, J. Hasegawa, M. Ishida, T. Nakajima, Y. Honda, O. Kitao, H. Nakai, M. Klene, X. Li, J. E. Knox, H. P. Hratchian, J. B. Cross, V. Bakken, C. Adamo, J. Jaramillo, R. Gomperts, R. E. Stratmann, O. Yazyev, A. J. Austin, R. Cammi, C. Pomelli, J. W. Ochterski, P. Y. Ayala, K. Morokuma, G. A. Voth, P. Salvador, J. J. Dannenberg, V. G. Zakrzewski, S. Dapprich, A. D. Daniels, M. C. Strain, O. Farkas, D. K. Malick, A. D. Rabuck, K. Raghavachari, J. B. Foresman, J. V. Ortiz, Q. Cui, A. G. Baboul, S. Clifford, J. Cioslowski, B. B. Stefanov, G. Liu, A. Liashenko, P. Piskorz, I. Komaromi, R. L. Martin, D. J. Fox, T. Keith, M. A. Al-Laham, C. Y. Peng, A. Nanayakkara, M. Challacombe, P. M. W. Gill, B. Johnson, W. Chen, M. W. Wong, C. Gonzalez, and J. A. Pople (Gaussian, Inc., Wallingford, CT, 2004).
[83] J. Paldus and X. Z. Li, Collect. Czech. Chem. Commun. **69**, 90 (2004).
[84] B. Ostojic and W. Domcke, Chem. Phys. **269**, 1 (2001).
[85] R. McDiarmid, Chem. Phys. Lett. **188**, 423 (1992).
[86] R. McDiarmid, J. Chem. Phys. **64**, 514 (1976).
[87] W. M. Flicker, O. A. Mosher, and A. Kuppermann, Chem. Phys. Lett. **45**, 492 (1977).
[88] T. Fujii *et al.*, Chem. Phys. Lett. **115**, 369 (1985).
[89] L. Serrano-Andres *et al.*, J. Phys. Chem. **97**, 9360 (1993).